A New Frontier in Ionospheric Observations: GPS Total Electron Content Measurements from Ocean Buoys

Irfan Azeem[1], Geoff Crowley[2], Victoriya Forsythe[1], Adam Reynolds[3], Erik Stromberg[1], Gordon R. Wilson[4], and Craig A Kohler[5]

[1]ASTRA LLC.
[2]Atmospheric and Space Technology Research Associates, 12703 Spectrum Drive, Suite 101,San Antonio, TX 78249, USA.
[3]ASTRA
[4]Air Force Research Laboratory
[5]National Oceanic and Atmospheric Administration

November 26, 2022

Abstract

Ground-based Global Navigation Satellite System (GNSS) receivers have become an ubiquitous tool for monitoring the ionosphere. Total Electron Content (TEC) data from globally distributed networks of ground-based GNSS receivers are increasingly being used to characterize the ionosphere and its variability. The deployment of these GNSS receivers is currently limited to landmasses. This means that 7/10 of Earth's surface, which is covered by the oceans, is left unexplored for persistent ionospheric measurements. In this paper, we describe a new low-power dual-frequency Global Positioning System (GPS) receiver, called Remote Ionospheric Observatory (RIO), which is capable of operating from locations in the air, space, and the oceans as well as on land. Two RIO receivers were deployed and operated from the Tropical Atmosphere Ocean buoys in the Pacific Ocean, and the results are described in this paper. This is the first time that GPS receivers have been operated in open waters for an extended period of time. Data collected between September 1, 2018 and December 31, 2019 are shown. The observed TEC exhibits a clear seasonal dependence characterized by equinoctial maxima in the data at both locations. Both RIO receivers, deployed near the geomagnetic equator, show an 18-35% increase in TEC during moderately disturbed geomagnetic periods. Comparisons with the International Reference Ionosphere model show good agreement. The new capability presented in this paper addresses a critical gap in our ability to monitor the ionosphere from the seventy percent of the Earth's surface that is covered by water.

A New Frontier in Ionospheric Observations: GPS Total Electron Content Measurements from Ocean Buoys

I. Azeem[1], G. Crowley[1], V. V. Forsythe[1], Adam Reynolds[1], Erik Stromberg[1], G. R. Wilson[2], and C. A. Kohler[3]

[1]Atmospheric & Space Technology Research Associates LLC., Louisville, CO, USA.

[2]Air Force Research Laboratory, Kirtland AFB, NM, USA.

[3]National Oceanic and Atmospheric Administration, National Data Buoy Center, Stennis Space Center, MS

Corresponding author: Irfan Azeem (iazeem@astraspace.net)

Key Points:

- A new capability for measuring Total Electron Content (TEC) from the ocean surface is presented.
- First measurements of TEC from two surface buoys in the Pacific Ocean are described.
- TEC enhancements in the equatorial region during moderate geomagnetic storms are observed.

Abstract

Ground-based Global Navigation Satellite System (GNSS) receivers have become an ubiquitous tool for monitoring the ionosphere. Total Electron Content (TEC) data from globally distributed networks of ground-based GNSS receivers are increasingly being used to characterize the ionosphere and its variability. The deployment of these GNSS receivers is currently limited to landmasses. This means that 7/10th of Earth's surface, which is covered by the oceans, is left unexplored for persistent ionospheric measurements. In this paper, we describe a new low-power dual-frequency Global Positioning System (GPS) receiver, called Remote Ionospheric Observatory (RIO), which is capable of operating from locations in the air, space, and the oceans as well as on land. Two RIO receivers were deployed and operated from the Tropical Atmosphere Ocean buoys in the Pacific Ocean, and the results are described in this paper. This is the first time that GPS receivers have been operated in open waters for an extended period of time. Data collected between September 1, 2018 and December 31, 2019 are shown. The observed TEC exhibits a clear seasonal dependence characterized by equinoctial maxima in the data at both locations. Both RIO receivers, deployed near the geomagnetic equator, show an 18-35% increase in TEC during moderately disturbed geomagnetic periods. Comparisons with the International Reference Ionosphere model show good agreement. The new capability presented in this paper addresses a critical gap in our ability to monitor the ionosphere from the seventy percent of the Earth's surface that is covered by water.

Plain Language Summary

The upper levels of the atmosphere, from about 80 km to over 1000 km altitudes, collectively referred to as the ionosphere consists of partially ionized gas. An increasingly large amount of ionospheric data comes from ground-based receivers that passively benefit from the signals transmitted onboard the Global Navigation Satellite System (GNSS) constellations. One of the most useful datasets provided by these GNSS receivers is the Total Electron Content (TEC). Ground-based GNSS receivers are widely deployed all over the world and have become the workhorse for doing ionospheric research. However, to date the deployment of these GNSS receivers has been limited to landmasses, which leaves 70% of the Earth's surface covered by the oceans un-instrumented for ionospheric studies. In this paper, we describe a new low-power dual-frequency GPS receiver, called the Remote Ionospheric Observatory (RIO), which is capable of continuous operation from ocean buoys for extended periods of time. We present data from two RIO receivers deployed on buoys in the Pacific Ocean. The new capability described in this paper is anticipated to open up many new applications for passively monitoring the ionosphere from previously inaccessible regions, such as the ocean.

1 Introduction

A significant challenge in comprehensive characterization and predictive modeling of the ionosphere is the paucity of high-fidelity and globally-distributed data. The dearth of ionospheric data is most acute in the regions covered by open ocean waters. Our ability to monitor the geospace environment from the ocean remains a technological challenge. This is a problem because the oceans cover about 70% of the Earth's surface. Traditional instruments used for ionospheric monitoring, such as ionosondes, all-sky imagers, and radars are too bulky and power intensive to be deployed on resource-limited ocean buoys. Thus far, these instruments have not been demonstrated to successfully operate from buoys in open waters. Even smaller and lower-power instruments, such as dual-frequency Global Navigation Satellite System (GNNSS) receivers, have not been utilized for routine operations from buoys. New sensor modalities that can operate from surface buoys are needed to address this critical gap in our observational capability and which, if successful, will open the way for innovative research activities.

Presently, the only means to monitor the ionosphere over the oceans is from satellites. The majority of ionospheric data from space-based platforms since the 1990s has come from satellite missions in Low Earth Orbit (LEO). Notable examples of satellite missions that have contributed ionospheric Total Electron Content (TEC) or electron density profile (EDP) measurements include TOPEX/Poseidon [Robinson and Beard, 1995; Codrescu et al., 1999], Constellation Observing System for Meteorology, Ionosphere, and Climate (COSMIC) [Schreiner et al., 2007; Lei et al., 2007], and now the COSMIC-2 mission [Schreiner et al., 2020]. Recently, several commercial providers, such as Spire and GeoOptics, are also providing TEC/EDP measurements from their respective constellations of GNSS Radio Occultation (RO) satellites [Forsythe et al., 2020]. These satellite missions share one pertinent characteristic; they all are in LEO. Due to their motion relative to a fixed point on Earth, LEO satellites are unable to provide persistent observations over a given geographic location. As a result, the observed ionospheric fluctuations in the data cannot be unambiguously deconvolved and attributed to spatial and temporal geophysical variations.

Over the last decade, TEC measurements from dense networks of GNSS receivers worldwide have provided an important database to study the ionosphere. GNSS receivers have enabled researchers to create TEC maps to study ionospheric responses to geomagnetic and lower atmospheric disturbances [Azeem et al., 2017a, b; Coster et al., 2017; Crowley et al., 2016; Occhipinti et al., 2013; Tsugawa et al., 2007; Komjathy, 1997; Mannucci et., 1998]. To date, these networks of GNSS receivers have only been deployed on land. This state of affairs is represented in Figure 1, which shows the current typical TEC coverage (red pixels) from publicly available ground-based dual frequency GPS receivers (black circles). Figure 1 also shows the locations of the two GPS receivers, called Remote Ionospheric Observatory (RIO), in the Pacific Ocean that are the focus of this study. We describe the RIO receiver in more detail in Section 2. From the figure it is abundantly clear that most TEC measurements come predominantly from the United States, South America, Europe, Japan and Australia. The gaps in data coverage are primarily seen in Africa, the Middle East, Asia, Antarctica, and the oceans. In this paper, we present a new capability for ionospheric remote sensing using GPS receivers designed specifically for operation from ocean buoys that could potentially be deployed globally.

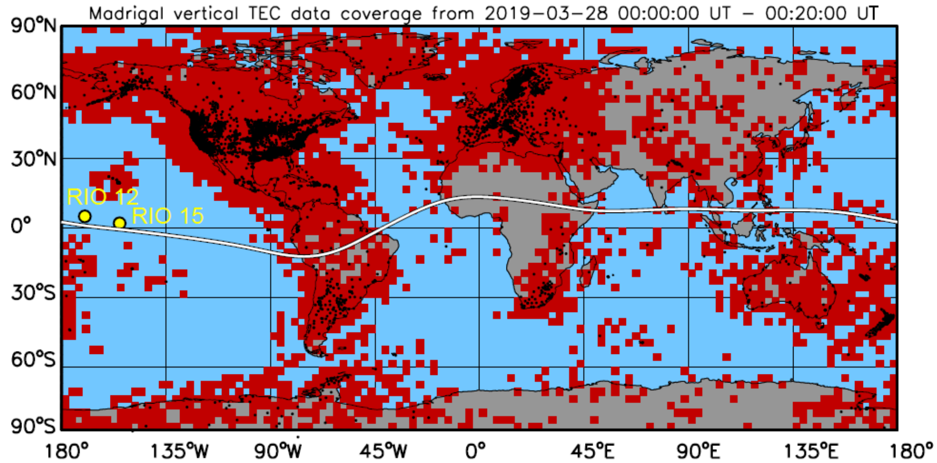

Figure 1. TEC coverage map with the locations of Ionospheric Pierce Points (IPP) shown in red and the locations of ground-based dual-frequency GPS receivers represented by black dots. The dearth of TEC coverage over the oceans is self-evident in the map. The yellow circles show the locations of the RIO receivers deployed on buoys. White line is the geomagnetic equator. The TEC map is generated using data from the Madrigal Database (http://millstonehill.haystack.mit.edu/).

In subsequent sections, we will provide a brief description of the small size, weight, and power (SwaP) RIO science-grade GPS receiver that is capable of operating autonomously from moored or tethered buoys. We will present TEC data from the pair of RIO GPS receivers that are deployed on the National Oceanic and Atmospheric Administration (NOAA) Tropical Atmosphere Ocean (TAO) buoys in the Pacific Ocean, as indicated in Figure 1. We will compare the TEC data with the International Reference Ionosphere 2016 (IRI-2016) model [Bilitza et al., 2017] for validation. The paper is organized as follows: the RIO GPS receiver systems on the buoys are introduced in Section 2; Section 3 describes the TEC data collected during field tests in Hawaii and Peru and initial validation comparisons with nearby ground-based GPS receivers; Section 4 discusses the TEC data from the TAO buoys collected over a 16-month period between September 1, 2018 and December 31, 2019 along with comparisons with the IRI-2016 model; Section 5 summarizes the conclusions of this study and examines the potential of ocean-based ionospheric monitoring capability for future ionospheric research.

2 Remote Ionospheric Observatory (RIO) GPS Receiver

RIO is a dual-frequency science-grade GPS receiver that tracks the traditional L1 (1.57542 GHz) civil signal (C/A, or Coarse/Acquisition code) and the L2 (1.22760 GHz) civil signal, L2C. RIO builds on the heritage of the CASES (Connected Autonomous Space Environment Sensor) receiver [Crowley et al., 2011; O'Hanlon, 2011], providing the same functionality as the original CASES GPS receiver but in a smaller package and with reduced power consumption. In contrast to CASES, the RIO GPS receiver uses only 2.5 W of power and is about 4.25”×4.5”×2.5” in length, width, and height. The RIO receiver design is optimized for operations in remote locations (including ocean deployments) where power and other resources may be extremely limited. Figure 2 shows the RIO GPS receiver in its current form as a commercial product.

Figure 2. RIO GPS receiver.

RIO samples the GPS L1 and L2C signals at 100 Hz and outputs fully processed TEC data nominally at 1 Hz (these data rates are programmable via a user configuration file). The amplitude (S_4) and phase scintillation (σ_ϕ) indices are also computed onboard the receiver, however, they are not presented in this paper as they are currently undergoing validation. In this study, we will focus on the TEC data from the two RIO receivers hosted on the NOAA TAO buoys.

The main RIO components include an RF Front End (RFE), a so-called mezzanine board, and a processor board. Figure 3 shows the block diagram of major components of the RIO GPS receiver. The RFE handles digitization of the data from the GPS antenna. It filters, amplifies, downconverts, samples, and packetizes the raw RF data for later processing. The mezzanine board includes a Field Programmable Gate Array (FPGA) for processing and a DC/DC converter for power management. The FPGA reads the raw digital samples from the RFE and buffers them for the processor board. It is also programmed to collect housekeeping data such as voltages, currents, and temperatures. The DC/DC converter manages power conversion and distribution to the rest of the boards in the system. The buffered RFE data is then fed to the processor board by the mezzanine. The processor board (onboard computer) is responsible for the GPS signal acquisition, tracking, navigation, scintillation and TEC calculation, etc. The processor board also interfaces with local data storage, network infrastructure, and any applicable communication radios, such as cell modems or satellite data modems.

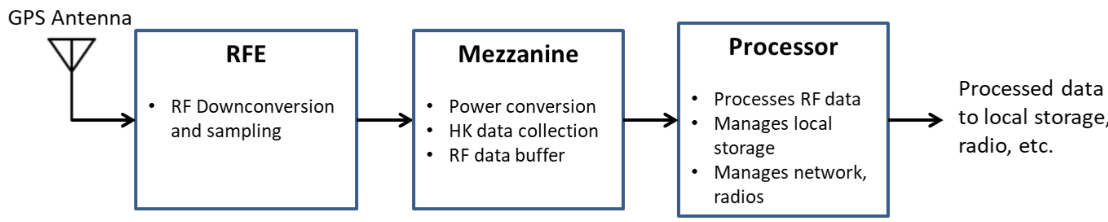

Figure 3. RIO block diagram with major components identified.

3 RIO GPS TEC Field Tests and Validation

The RIO GPS receiver underwent several ocean deployments in Hawaii and Peru for functional testing, validation, and verification. These tests and evaluations of the engineering units were used to finalize the RIO design, which is now deployed on the NOAA TAO buoys. In this Section, we briefly review the GPS TEC from the final field test in Peru and present comparisons of the data collected from the ocean surface to a nearby ground-based GPS receiver as a proof of validation.

For the sea trial off the coast of Peru, a RIO engineering unit was integrated on the Wave Glider autonomous surface vehicles (ASV) [Thomson, et al., 2018] and deployed 22 miles off the coast for 8 days under various ocean roughness conditions. The Wave Glider consists of two major systems: the floating buoy, and a motor that hangs from the bottom of the buoy. The 'motor' consists of a 'wing' mechanism that is driven simply by wave action, and can be steered by a rudder programmed from a computer on the buoy. Most of the infrastructure is contained in the floating buoy, which includes 'dry-box' compartments for various payloads, a dry-box for the command and control electronics, solar panels and various antennas. During the field test, the host Wave Glider was programmed to keep station at a reference location and telemetry signals were transmitted in real time via the Iridium satellite link to a ground site. This and previous tests (not shown here) also included a newer version of the CASES GPS receiver, called GAMMA, several of which were deployed on the ground within 1.5 mile of the shore and served to provide a stationary reference for comparisons with the measurements collected on the water.

The field test in Peru took place 20-27 January 2015 during which the host Wave Glider was programmed to perform various maneuvers that included station keeping about a reference point, straight-line transitions between two waypoints, and box pattern traversals. The TEC data shown in this Section were collected on January 21, 2015 when the Wave Glider was operating in a station keeping mode at 12.07° S, 77.47° W about 22 miles (~35 km) off the coast of Lima, Peru. During this test, a GAMMA GPS receiver was also deployed on the ground in Lima, Peru at 12.05° S, 77.12° W. Figure 4 shows the TEC measurements in units of TECU (1 TECU = 10^{16} $\#/m^{-2}$) from the RIO on the Wave Glider and the data from the land-based GAMMA GPS receiver in Lima. The different colored curves in Figure 4 represent several different GPS satellites tracked by the receivers. The TEC data from the land-based GAMMA is shown in Figure 4a, while the concurrently acquired RIO data is plotted in Figure 4b. The TEC measurements from RIO on the Wave Glider show good qualitative agreement with those from the reference ground-based GAMMA GPS receiver. One does not necessarily expect the two data sets to be identical since the ionosphere over Peru tends to contain a lot of variable structure, and the receivers were about 22 miles apart resulting in a slightly different Ionospheric Pierce Point (IPP) geometry. Nonetheless, the TEC measurements from the ground-based and ocean-deployed GPS receivers show similar variations and trends in the data. The overall agreement between the two datasets suggests that the RIO measurements from the buoy are comparable in quality to the ground-based TEC data. To better quantify this agreement, 1-min averaged TEC data from the Wave Glider and ground-based GAMMA are compared to each other in Figure 5. The correlation coefficient between the 5925 TEC data points compared is 0.98 showing extremely good agreement. As mentioned earlier, trials were performed over an 8-day interval and similar results were obtained every day.

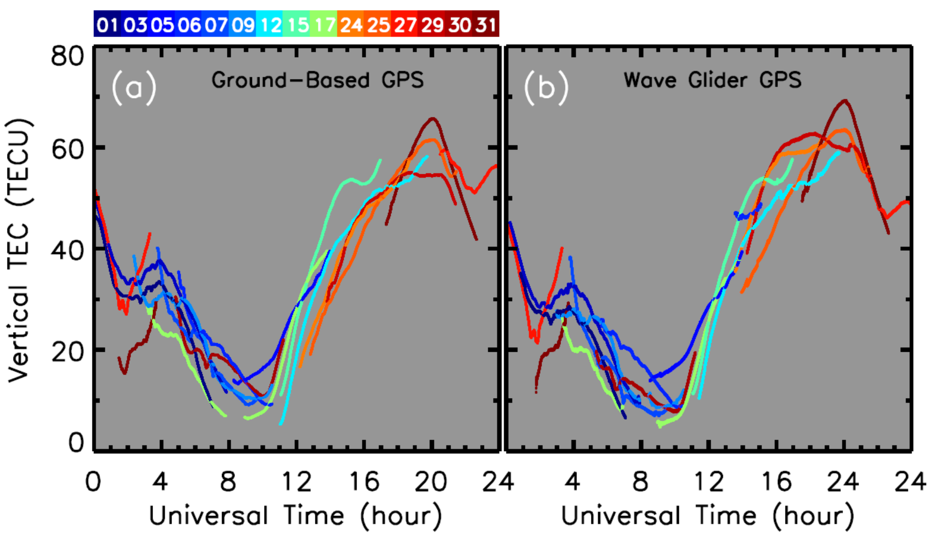

Figure 4. (a) TEC from a reference GAMMA GPS receiver located at Lima, Peru. (b) TEC from the RIO GPS receiver on the Wave Glider while deployed 22 miles off the coast of Lima. The color corresponds to the PRN of the GNSS satellite, shown on top of panel (a). The two time series exhibit similar trends and variations, which were interpreted as a validation of the data quality of the GPS receiver on the Wave Glider. The receiver bias in both data sets was estimated using the publicly-available IONEX global TEC data from the National Aeronautics and Space Administration (NASA) Crustal Dynamics Data Information System (ftp://cddis.nasa.gov/gnss/products/ionex/).

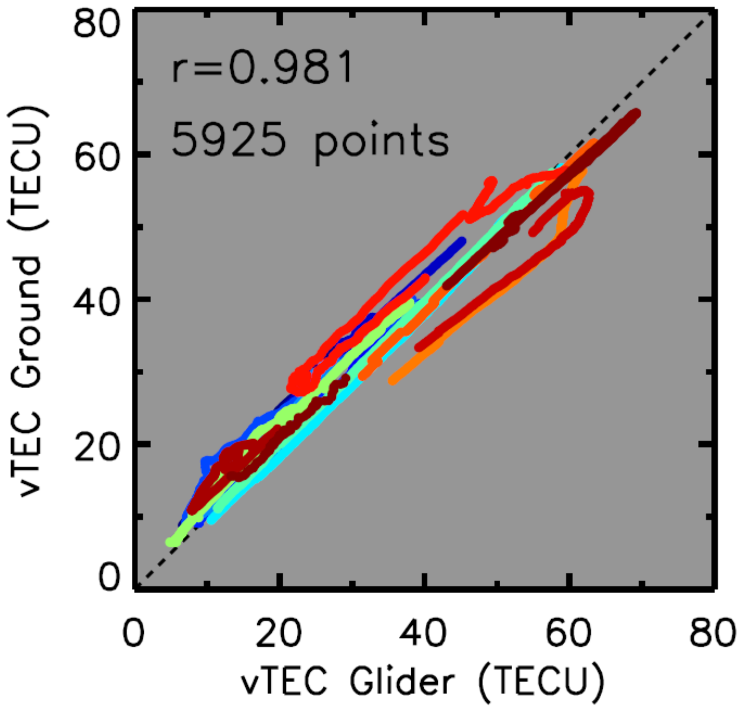

Figure 5. Comparison of vertical TEC (vTEC) measurements from the RIO GPS receiver on Wave Glider and the reference GAMMA GPS receiver located in Lima, Peru. The colors represent different PRNs as identified in Figure 4. Each data point is a 1-min average. The correlation coefficient between a total number of 5925 points is 0.981.

4 RIO Systems on NOAA TAO Buoys in the Pacific Ocean

In August 2018, two RIO receivers, hereafter referred to as RIO-12 and RIO-15, were deployed on the NOAA TAO buoys in the Pacific Ocean near the geographic equator. The locations of these buoys are shown in Figure 1. The TAO array [Hayes, 1991] consists of approximately 70 moored buoys in the tropical Pacific Ocean to provide ocean and atmospheric observations in support of El Niño/Southern Oscillation (ENSO) monitoring and prediction. The TAO array is operated by the NOAA National Data Buoy Center (NDBC). The TAO buoys are typically deployed in water depths between 1500 and 6000 m and each one consists of a 2.3 m diameter fiberglass/foam toroid, with an aluminum tower and a stainless steel bridle (see Figure 6).

Figure 6. NOAA TAO buoy similar to those hosting RIO GPS receivers in the Pacific Ocean.

While each TAO buoy includes data logging, telemetry, and battery systems to support various meteorological and hydrographic sensors, we only used them as platforms to mechanically host the RIOs. This was done deliberately so as not to interfere with the NOAA/NDBC's mission critical measurements. The RIO systems designed for the TAO buoys included their own telemetry, thermal management, and power subsystems, allowing them to operate independently of the other sensors and systems. Each RIO is housed in a weather-proof and corrosion-resistant enclosure along with an Iridium communication modem, an over-voltage protection system, low-power alarms, and an advanced power management controller to protect electronic equipment from catastrophic events. A solar panel (also rated for operations in the marine environment) was mounted on each of the three vertical faces of the aluminum tower, and a GPS antenna was affixed to the top ring of the TAO buoy. Figure 7 shows a drawing of the RIO GPS receiver's placement on the TAO buoy. The figure also shows the locations of the solar panels for recharging the RIO batteries.

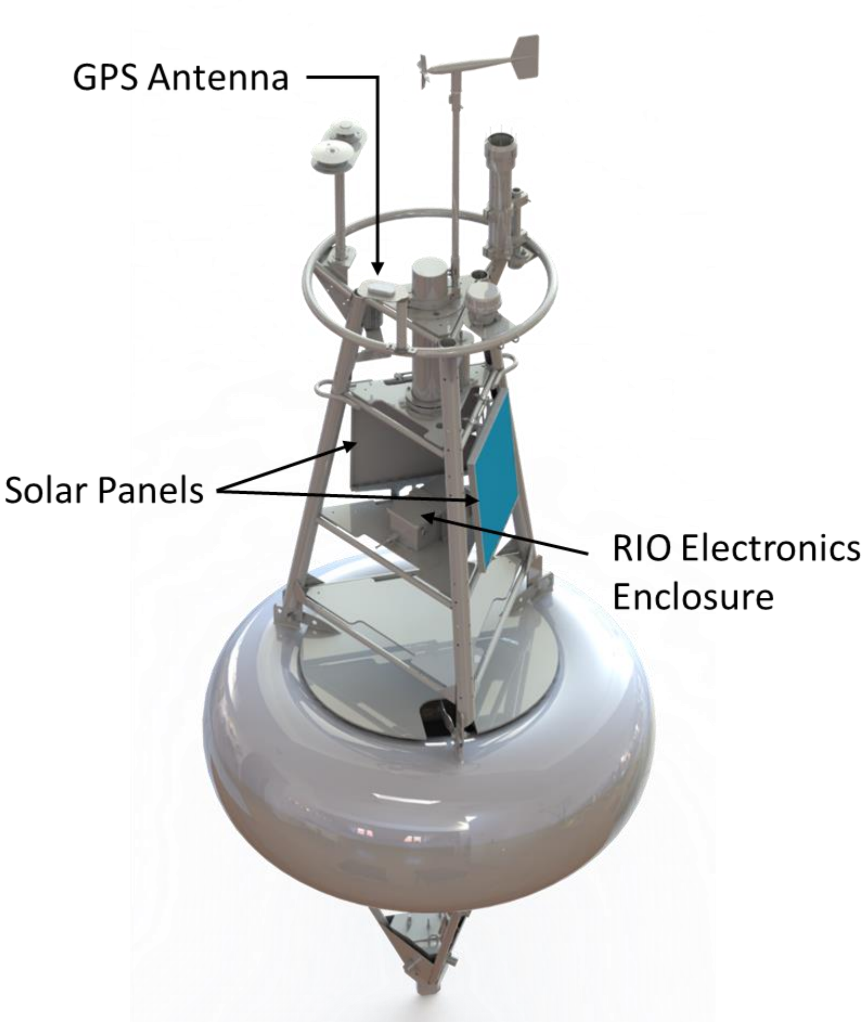

Figure 7. Computer rendering of the NOAA TAO buoy showing the placements of the RIO electronics enclosure, the GPS antenna, and two out of three solar panels.

Fully processed 1-min resolution TEC data from the RIO receivers on each of the TAO buoys are transmitted to a ground-side server over the Iridium link. The RIO data extraction strategy is as follows: Science and housekeeping data is continuously saved to a buffer on the RIO. Every 2 hours the data is transmitted to the server and the buffer is cleared. During routine operations, the transmitted packet would include TEC data from the last 2 hours. If, for any reason, a scheduled Iridium connection is not established successfully, the RIO processor would re-initiate the connection every hour until a link is established at which point all buffered data is transmitted. The chosen connection period of 2 hours is driven entirely by the need to reduce the incurred Iridium data charges and is not an attribute of any technical requirements or impediments. If desired, the data could be returned in near real-time for operational campaigns.

5 Results

In this section we present summary plots of the TEC data from RIO-12 and RIO-15 collected between September 1, 2018 and December 31, 2019. These summary plots show 5-minute averaged TEC data from all available GPS satellites. The averaging was done to reduce high-frequency noise in the TEC data. For visual clarity, we show two sets of summary plots for each RIO receiver; one plot covering September 1, 2018 through December 31, 2018 and the other for the entire year of 2019. Only TEC values obtained above 20° elevations are used in generating these summary plots. The 10.7 cm solar radio flux ($F_{10.7}$) during this observation period was representative of solar minimum conditions. The 81-day running mean of the daily $F_{10.7}$ over the data collection period is shown in Figure 8. The prevailing solar minimum conditions make this dataset ideal for studying ionospheric responses to external drivers, such as geomagnetic storms.

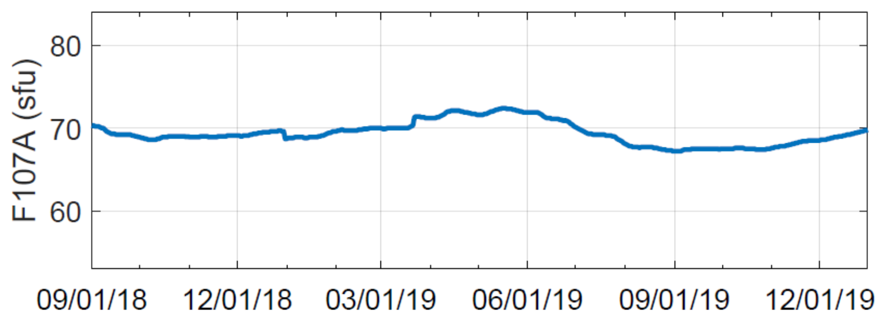

Figure 8. 81-day running mean of the daily F10.7 index between September 1, 2018 and December 31, 2019.

5.1 TEC from RIO-12 and RIO-15 GPS Receivers

Figure 9 shows the local time (LT) variations of the measured TEC between September 1, 2018 and December 31, 2018 from RIO-12 and RIO-15. The figure also shows the Dst and Kp indices during the same period. It is worth reminding ourselves that RIO-12 is deployed near 5° N while the RIO-15 host buoy is moored near 2° N. The geomagnetic latitudes of RIO-12 and RIO-15 are 3.73° N and 3.4° N, respectively. The buoys are separated by about 1800 km in the East-West direction. While there exist subtle differences in the data from the two locations, in this section we focus on the main features of the TEC measurements that are common to both datasets. Both receivers show the dayside increase in TEC between 10 and 18 LT, driven by the plasma generation from solar illumination. On average, the peak daytime TEC values are about 30 TECU during the equinox months (September-November) and 22 TECU during December. Figure 10 shows year-long TEC measurements from RIO-12 and RIO-15 in 2019. As with Figure 9, the daytime TEC increase is clearly evident between 10 and 18 LT in both datasets. These year-long datasets also reveal a clear seasonal variation with values during solstices generally being lower than during the equinox months.

An inspection of the Dst and Kp data in Figures 9 and 10 reveals several moderate geomagnetic storms (Dst ~ -50 nT) interspersed throughout the observation period of this study.

A clear association between TEC enhancements and Dst excursions during storm times is apparent in the figures. The TEC is seen to increase rapidly at the storm onset and remains elevated for at least several days during the recovery period. This behavior of TEC during storm times has been reported previously [Lei et al., 2014; Heelis, 2008; Mannucci et al., 2005; Buonsanto, 1999]. The main driver of the storm-time increase in the dayside TEC is the eastward directed prompt penetration electric field of magnetospheric origin and the associated upward **E** × **B** drifts at the equator, which lifts the plasma upward and raises the layer to altitudes where recombination rates are low [Mannucci et al., 2005].

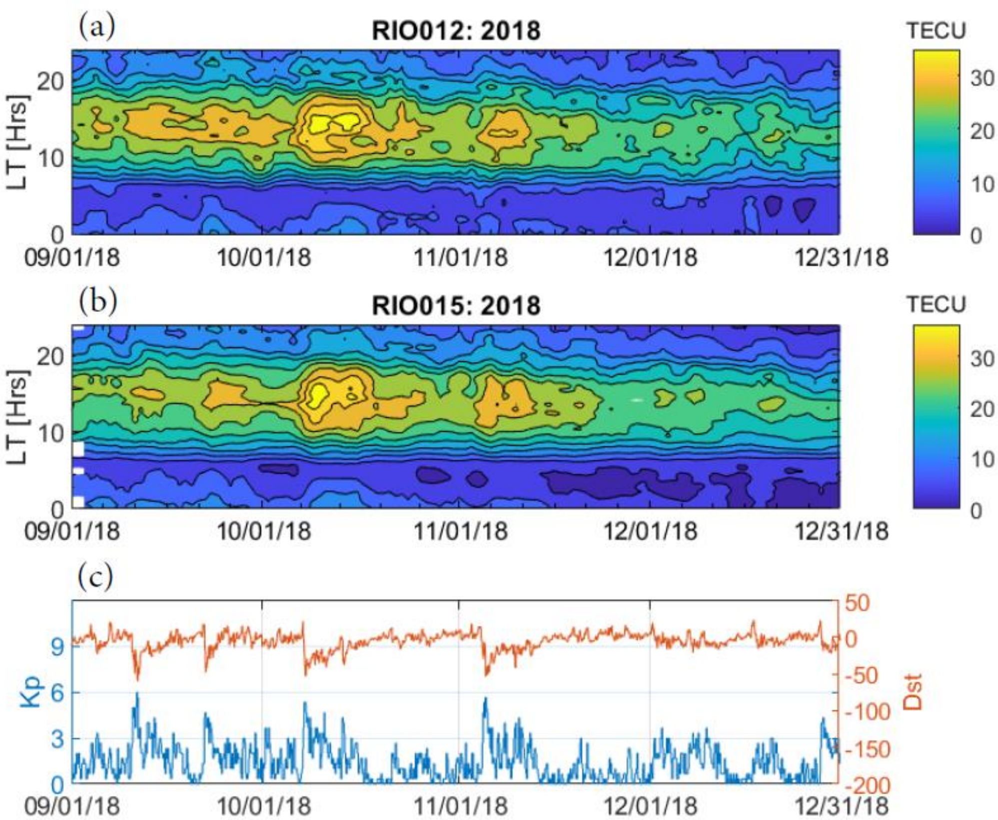

Figure 9. TEC data from (a) RIO-12 and (b) RIO-15 GPS receivers between September 1, 2018 and December 31, 2018. (c) Dst and Kp indices during this period. Several moderate storms are evident in the Dst and Kp data.

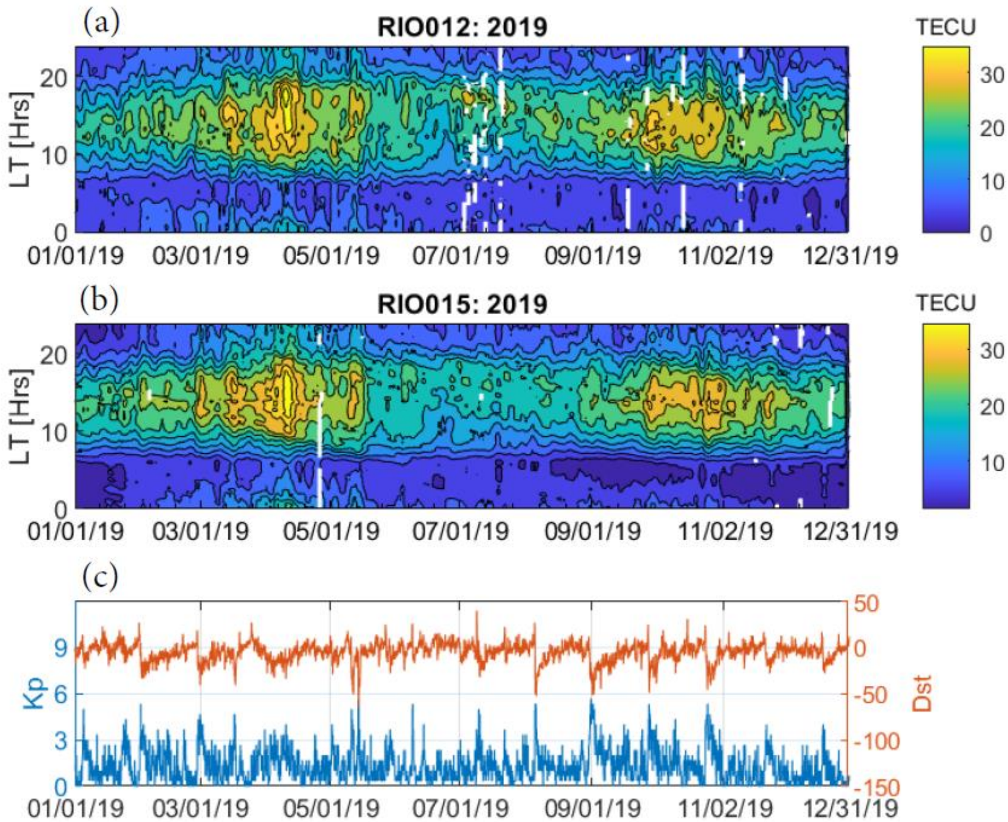

Figure 10. Same as Figure 9 but for TEC data collected between January 1, 2019 and December 31, 2019.

Figure 11 shows seasonally-averaged LT variations in the 5-min averaged TEC data from RIO-12. These seasonal averages were formed using all available data between September 2018 and December 2019. The gray-shaded regions represent 1σ standard deviation. Comparing the peak TEC values across different panels in Figure 11, we observe that there are annual and semiannual variations with maxima near the equinoxes, a primary minimum near the June solstice, and a secondary minimum near the December solstice. Similar annual/semiannual variations have been reported in the daytime low latitude *NmF2* and *hmF2* data from the COSMIC mission by Burns et al. [2012]. Similar seasonal averages were computed for RIO-15, which show identical features and therefore are not shown here. There are clear differences in the LT variation between different seasons, which will be examined in detail in a future study. Here, we simply note that the spring equinox and summer solstice daytime TEC tend to have a flatter LT response in contrast to the fall and winter daytime TEC, which exhibit a steeper rise and roll off.

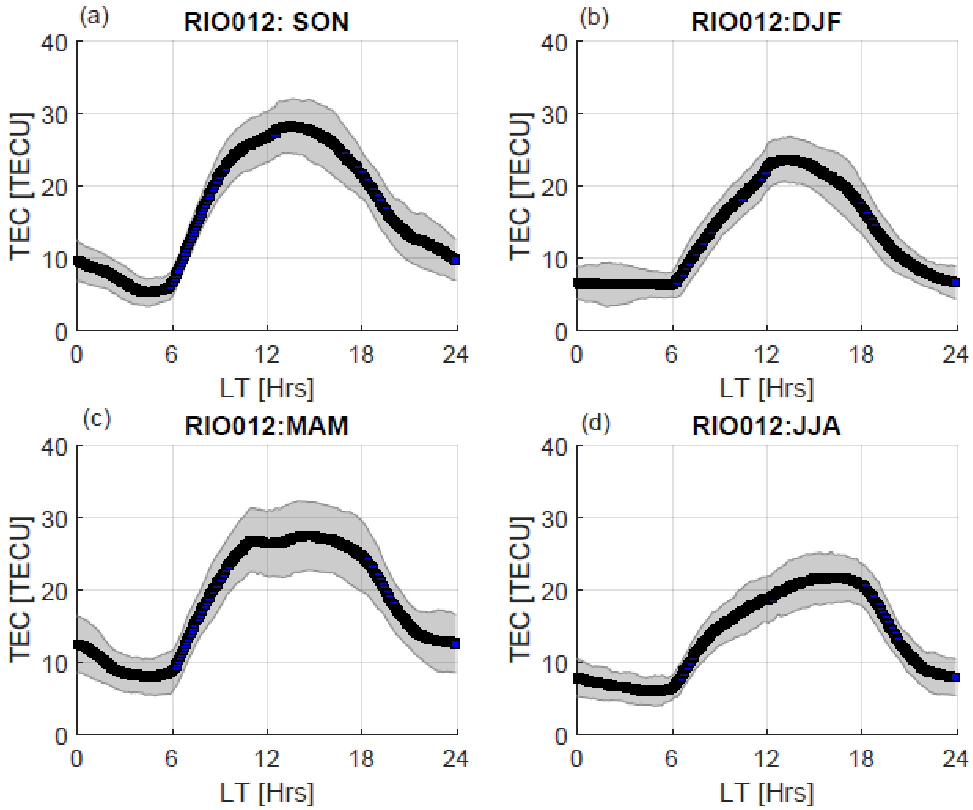

Figure 11. Seasonally-averaged local time variations of TEC from the RIO-12 GPS receiver for (a) fall equinox, (b) winter solstice, (c) spring equinox, and (d) summer solstice. The gray shaded region in each of the panels represent 1σ standard deviation.

5.3 Comparisons with IRI-2016

To assess the overall data quality from the RIO receivers, we compared the RIO-12 and RIO-15 TEC measurements with the International Reference Ionosphere 2016 (IRI-2016) [Bilitza et al., 2017]. Figures 12a and 12b show comparisons between the IRI-2016 model and hourly averaged RIO-12 and RIO-15 TEC data, respectively. The overall agreement with the IRI model is very good, with correlation coefficients of 0.902 and 0.890 for RIO-12 and RIO-15, respectively. On closer inspection, the scatter plots in Figure 12 show a difference between the daytime and nighttime comparison. The majority of low TEC values (corresponding to nighttime measurements) are located below the dashed diagonal line, meaning the night-time RIO TEC values tend to be 2-5 TECU higher than the IRI-2016 model results. On the other hand, the daytime measurements of TEC are about 5-6 TECU lower than the IRI-2016 TEC values.

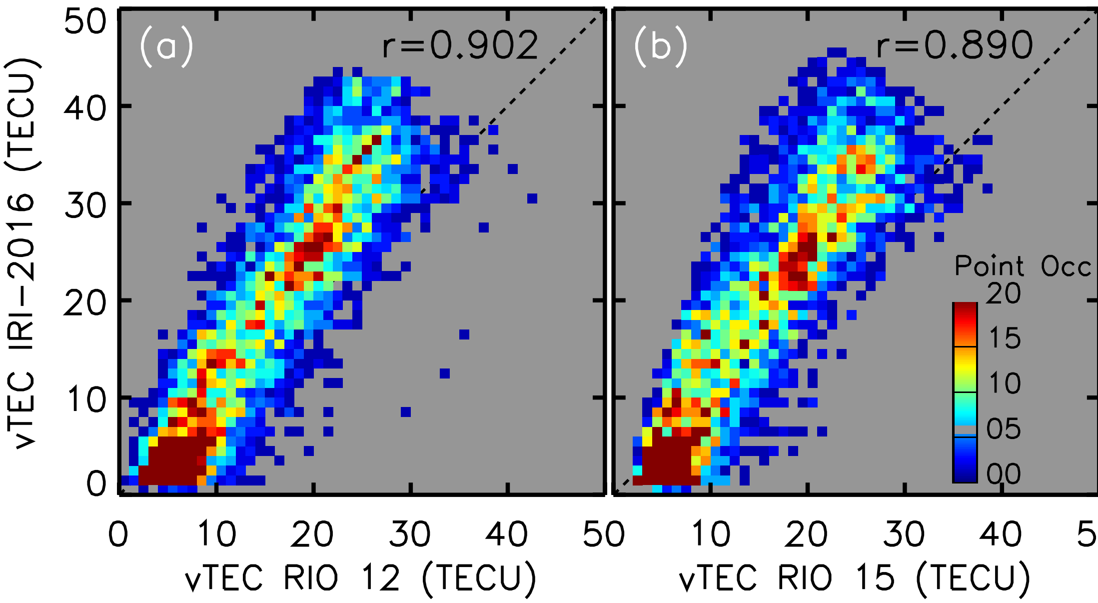

Figure 11. Comparison between hourly averaged TEC from (a) RIO-12, (b) RIO-15 GPS receivers and IRI-2016 TEC. The colors represent different data point occurrences in accordance with the color bar shown in panel (b). The total number of data points compared are 5755 and 5771 for RIO-12 and RIO-15, respectively. The linear correlation coefficients are shown at the top of the panels.

We further compare the IRI-2016 and RIO TEC measurements by computing their differences and binning the differences in magnetic local time (MLT) to examine the distributions. Figure 13 (a) and (b) show histograms of data/model differences computed for RIO-12 and RIO-15, respectively. The shapes of both histograms suggest that there are two underlying Gaussian distributions. One distribution has a peak below zero and the other is centered above zero. This split is indeed due to the diurnal variation of TEC. Figures 13 (c) and (d) show the histograms of RIO and IRI TEC differences binned for different MLT sectors. These figures now clearly show that the IRI-2016 underestimates the measured TEC during the night time (18-03 MLT) and overestimates it during the day time (09-18 MLT).

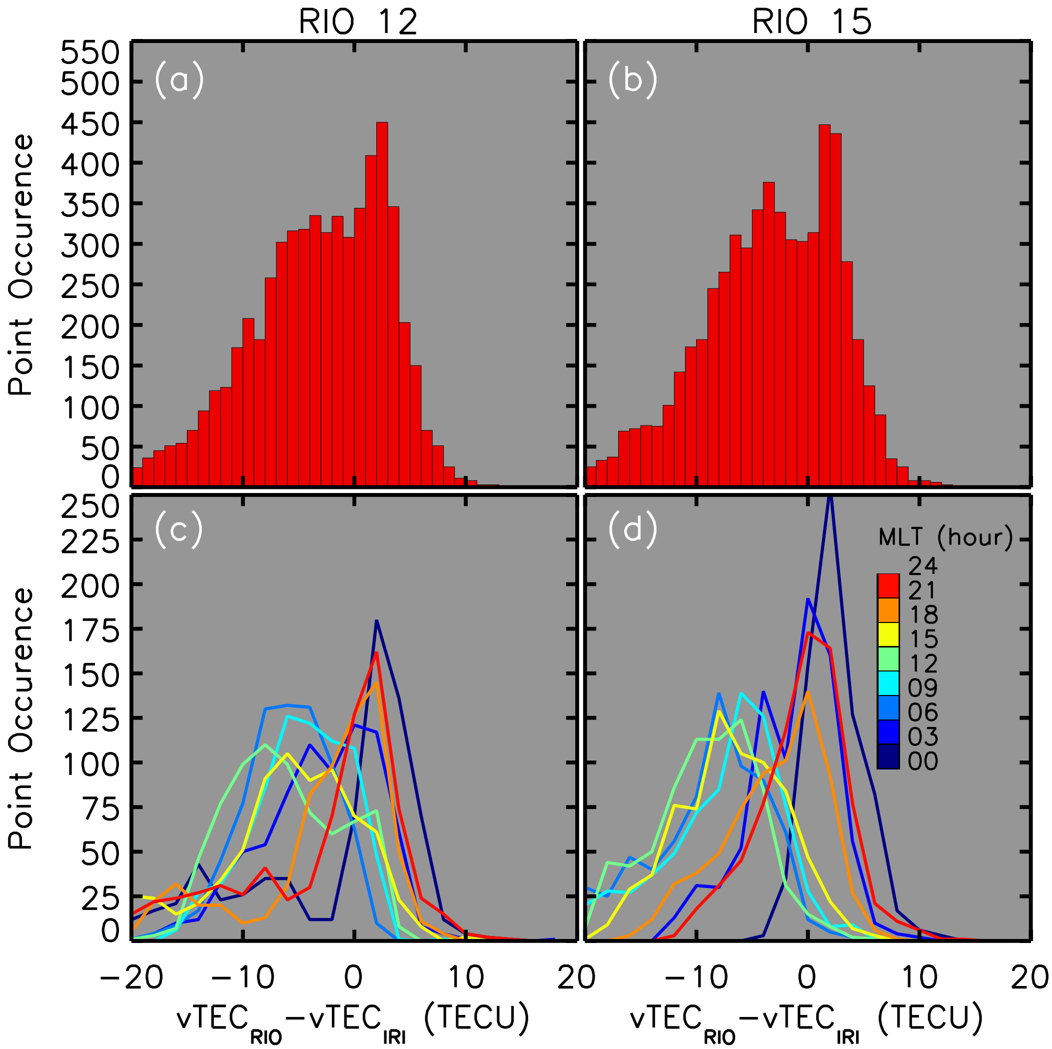

Figure 12. Differences between the TEC from the IRI-2016 model and (a) RIO-12 and (b) RIO-15. Panels (c) and (d) show the differences binned in MLT, indicated by the color with the color bar shown in panel (d).

6 Conclusions

Our ability to continuously monitor the ionosphere from the vast stretches of open water remains a technological challenge. This is a problem because oceans cover about 70% of the Earth's surface. Ocean-based ionospheric monitoring, heretofore, has not been possible due to the harsh environment and logistical challenges in deploying sensors on resource-constrained buoys. Additionally, the constant motion imparted by ocean waves to the buoy further complicates the GPS signal acquisition, tracking, and processing. Currently, there are no viable methods of receiving and processing GPS TEC information from a platform in the ocean. This leaves 7/10th of Earth without adequate observational coverage for ionospheric studies. Addressing this observational gap is particularly crucial for measuring ionospheric variability globally. In this paper, we have demonstrated the feasibility of making high fidelity GPS TEC measurements from ocean-based platforms, such as moored and mobile buoys. We describe the RIO GPS receiver, with its small SWaP design and software features, capable of operating autonomously from resource-constrained ocean surface buoys. We also present our concept of operation for the RIO receivers deployed on NOAA TAO buoys in the Pacific Ocean. The data quality and reliability from the RIO receivers on TAO buoys are comparable to those from ground-based GPS receivers. A preliminary analysis of the TEC data collected from the buoys, which are located near the magnetic equator, shows two key findings:

1) The observed TEC exhibits a clear seasonal dependence characterized by equinoctial maxima.

2) Moderate geomagnetic storms are associated with the observed daytime TEC enhancements.

This is the first time that GPS receivers have been deployed and operated in open waters for an extended period of time. This study serves as a proof of concept demonstration that continuous GPS TEC measurements can be reliably made from ocean buoys. In the future, small SWaP GPS receivers, such as RIO, can be (and should be) deployed on arrays of ocean buoys to complement the distributed networks of ground-based GPS receivers. The long-term vision of this work is to enable continuous and persistent observations from distributed sensors, both from ground-based and ocean platforms, to provide the much needed data to resolve and quantify a variety of temporal and spatial scales of ionospheric variability. In summation, this study of GPS TEC measurements from the NOAA TAO buoys demonstrates that the ocean-based observation modality represents a new frontier in ionospheric remote sensing, which can open the way for new research activities in the geospace community.

Acknowledgments

This study was supported by the Air Force Small Business Innovation Research (SBIR) contract FA9453-13-C-0035 to ASTRA. IA acknowledges support from Liquid Robotics Inc., Sunnyvale, CA during the integration of RIO GPS receivers on Wave Gliders and the execution of field tests in Hawaii and Peru. TAO host buoys for the RIO deployments were provided by NOAA/NDBC. The source code of IRI-2016 model is available at http://irimodel.org. The GPS TEC data from TAO buoys are available at https://doi.org/10.5281/zenodo.3903770.

References

Azeem, I. and M. Barlage, Atmosphere-Ionosphere Coupling from Convectively Generated Gravity Waves, Adv. Space Res. (2017a), https://doi.org/10.1016/j.asr.2017.09.029.

Azeem, I., S. L. Vadas, G. Crowley, and J. J. Makela (2017b), Traveling ionospheric disturbances over the United States induced by gravity waves from the 2011 Tohoku tsunami and comparison with gravity wave dissipative theory, J. Geophys. Res. Space Physics, 122, doi:10.1002/2016JA023659.

Bilitza, D., D. Altadill, V. Truhlik, V. Shubin, I. Galkin, B. Reinisch, and X. Huang (2017), International Reference Ionosphere 2016: From ionospheric climate to real-time weather predictions, Space Weather, 15, 418-429, doi:10.1002/2016SW001593.

Buonsanto, M. Ionospheric Storms — A Review. *Space Science Reviews* **88,** 563–601 (1999). https://doi.org/10.1023/A:1005107532631

Burns, A. G., S. C. Solomon, W. Wang, L. Qian, Y. Zhang, and L. J. Paxton (2012), Daytime climatology of ionospheric NmF2 and hmF2 fromCOSMIC data, J. Geophys. Res., 117, A09315, doi:10.1029/2012JA017529.

Codrescu, M. V., S. E. Palo, X. Zhang, T. J. Fuller-Rowell, C. Poppe (1999), TEC climatology derived from TOPEX/Poseidon measurements, J. Atmos. Sol. Terr. Phys., 61(3-4), 281-298, https://doi.org/10.1016/S1364-6826(98)00132-1.

Coster, A. J., Goncharenko, L., Zhang, S.-R., Erickson, P. J., Rideout, W., & Vierinen, J. (2017). GNSS observations of ionospheric variations during the 21 August 2017 solar eclipse. Geophysical Research Letters, 44, 12,041– 12,048. https://doi.org/10.1002/2017GL075774.

Crowley, G., G. S. Bust, A. Reynolds, I. Azeem, R. Wilder, B. W. O'Hanlon, M. L. Psiaki, S. Powell, T. E. Humphreys, and J. A. Bhatti (2011), CASES: A Novel Low-Cost Ground-based Dual-Frequency GPS Software Receiver and Space Weather Monitor, Proceedings of ION GNSS, Portland, Oregon.

Crowley, G., I. Azeem, A. Reynolds, T. M. Duly, P. McBride, C. Winkler, and D. Hunton (2016), Analysis of traveling ionospheric disturbances (TIDs) in GPS TEC launched by the 2011 Tohoku earthquake, Radio Sci., 51, 507–514, https://doi:10.1002/2015RS005907.

Forsythe, V. V., Duly, T., Hampton, D., & Nguyen, V., (2020), Validation of ionospheric electron density measurements derived from Spire CubeSat constellation. *Radio Science*, 55, https://doi.org/10.1029/2019RS006953.

Hayes, S. P., L. Mangum, J. Picaut, A. Sumi, and K. Takeuchi, 1991: TOGA-TAO: A Moored Array for Real-time Measurements in the Tropical Pacific Ocean. *Bull. Amer. Meteor. Soc.*, **72**, 339–347, https://doi.org/10.1175/1520-0477(1991)072<0339:TTAMAF>2.0.CO;2.

Heelis, R.A. (2013). Low- and Middle-Latitude Ionospheric Dynamics Associated with Magnetic Storms. In Midlatitude Ionospheric Dynamics and Disturbances (eds P.M. Kintner, A.J. Coster, T. Fuller-Rowell, A.J. Mannucci, M. Mendillo and R. Heelis). doi:10.1029/181GM06.

Komjathy, A. (1997), Global ionospheric total electron content mapping using the Global Positioning System, Ph.D. dissertation, Tech. Rep. 188, Dep. of Geodesy and Geomatics Eng., Univ. of New Brunswick, Fredericton, N. B., Canada.

Lei, J., et al. (2007), Comparison of COSMIC ionospheric measurements with ground-based observations and model predictions: Preliminary results, J. Geophys. Res., 112, A07308, doi:10.1029/2006JA012240.

Lei, J., W.Wang,A.G. Burns, X. Yue, X. Dou, X. Luan, S. C. Solomon, and Y. C.-M. Liu (2014), New aspects of the ionospheric response to the October 2003 superstorms from multiple-satellite observations, J. Geophys. Res. Space Physics, 119, doi:10.1002/2013JA019575.

Mannucci, A. J., B. D. Wilson, D. N. Yuan, C. H. Ho, U. J. Lindqwister, and T. F. Runge (1998), A global mapping technique for GPS-derived ionospheric electron content measurements, Radio Sci., 33, 565–582, doi:10.1029/97RS02707.

Mannucci, A. J., B. T. Tsurutani, B. A. Iijima, A. Komjathy, A. Saito, W. D. Gonzalez, F. L. Guarnieri, J. U. Kozyra, and R. Skoug (2005), Dayside global ionospheric response to the major interplanetary events of October 29–30, 2003 ‘‘Halloween Storms,’’ Geophys. Res. Lett., 32, L12S02, doi:10.1029/2004GL021467.

Occhipinti, G., L. Rolland, P. Lognonne, and S. Watada (2013), From Sumatra 2004 to Tohoku Oki 2011: The systematic GPS detection of the ionospheric signature induced by tsunamigenic earthquakes, J. Geophys. Res. Space Physics, 118, 3626– 3636, doi:10.1002/jgra.50322.

O’Hanlon, B.W., M.L. Psiaki, S. Powell, J. A. Bhatti, T.E. Humphreys, G. Crowley, and G.S. Bust (2011), CASES: A Smart, Compact GPS Software Receiver for Space Weather Monitoring, Proc. of the 24th International Technical Meeting of The Satellite Division of the Institute of Navigation, Portland, OR, 2745-2753

Robinson, T. R. and R. Beard (1995), A comparison between electron content deduced from the IRI and that measured by the TOPEX dual frequency altimeter, Adv. Space Res., 16(1), 155-158, https://doi.org/10.1016/0273-1177(95)00116-V.

Schreiner, W., C. Rocken, S. Sokolovskiy, S. Syndergaard, and D. Hunt (2007), Estimates of the precision of GPS radio occultations from the COSMIC/FORMOSAT-3 mission, Geophys. Res. Lett., 34, L04808, doi:10.1029/2006GL027557.

Schreiner, W. S., Weiss, J. P., Anthes, R. A., Braun, J., Chu, V., Fong, J., et al. (2020). COSMIC-2 radio occultation constellation: First results. *Geophysical Research Letters*, 47, e2019GL086841. https://doi.org/10.1029/2019GL086841.

Thomson, J., J. B. Girton, R. Jha, and A. Trapani (2018), Measurements of Directional Wave Spectra and Wind Stress from a Wave Glider Autonomous Surface Vehicle. *J. Atmos. Oceanic Technol.*, **35**, 347–363, https://doi.org/10.1175/JTECH-D-17-0091.1.

Tsugawa, T., Y. Otsuka, A. J. Coster, and A. Saito (2007), Medium-scale traveling ionospheric disturbances detected with dense and wide TEC maps over North America, Geophys. Res. Lett., 34, L22101, doi:10.1029/2007GL031663.